2018 IEEE/RSJ International Conference on Intelligent Robots and Systems (IROS)
Madrid, Spain, October 1-5, 2018

Design and Fabrication of a Bipedal Robot using Serial-Parallel Hybrid Leg Mechanism

Kevin G. Gim, Joohyung Kim, and Katsu Yamane

Abstract— **In this paper, we present the design and performance evaluation of a bipedal robot that utilizes the Hybrid Leg mechanism. It is a leg mechanism that achieves 6 DOF with a combined structure of serial and parallel mechanism. It is designed to have a light structural inertia and large workspace for agile bipedal locomotion. A new version of Hybrid Leg is fabricated with carbon fiber tubes and bearings to improve its structural rigidity and accuracy while supporting its weight. A pair of Hybrid Legs is assembled together for bipedal locomotion. In the assembly, we adopt a pelvis structure with an yaw angle offset to enlarge the feet workspace, inspired by the toe-out angle of the human feet. The workspace and range of velocity are presented in simulation and verified with hardware experiments. We also demonstrate a simple forward walking motion with the developed robot.**

I. Introduction

Bipedal locomotion is one of the most important features of humanoid robots. While a large body of work has been devoted to bipedal locomotion control in order to improve its agility and stability, there is small variety in mechanism design of the leg structure. Most bipedal robots adopt 6-degrees-of-freedom (DOF) serial mechanism (3 DOF hip joint, 1 DOF knee pitch joint, and 2 DOF ankle joint) for their legs because of its similarity to human limbs as well as straightforward structure, large workspace, and simple manufacturing and maintenance processes. Many humanoid platforms [1]–[4] had been developed with the 6-DOF serial leg mechanism and a majority of recent humanoid robots, e.g. the robots developed for DARPA Robotics Challenge [5]–[9], also adapted this leg mechanism.

In contrast, a few researchers have incorporated parallel mechanism into serial structure to take advantage of both mechanisms. Most of such designs apply parallel mechanism to an ankle structure in order to realize compact ankle joint and small leg inertia by bringing the actuator closer to the hip. For example, the leg of humanoid robot LOLA has a typical 6-DOF serial structure but the 2 DOF ankle joint is actuated by two spatial slider-crank mechanism instead of placing two actuators at the ankle joint [10]. WALK-MAN, a humanoid robot developed at IIT, also applied 4-bar transmission to its knee and ankle joints to reduce the inertia and maximize its dynamic performance [11].

Furthermore, some bipedal walking platforms with parallel mechanism legs successfully achieved agile and dynamic locomotion. ATRIAS designed their leg with co-axial double motor with 4-bar linkage mechanisms to minimized the leg mass and inertia [12]. The leg design of a commercialized bipedal platform CASSIE also consists of multiple 4-bar linkage mechanisms [13] for the similar purpose.

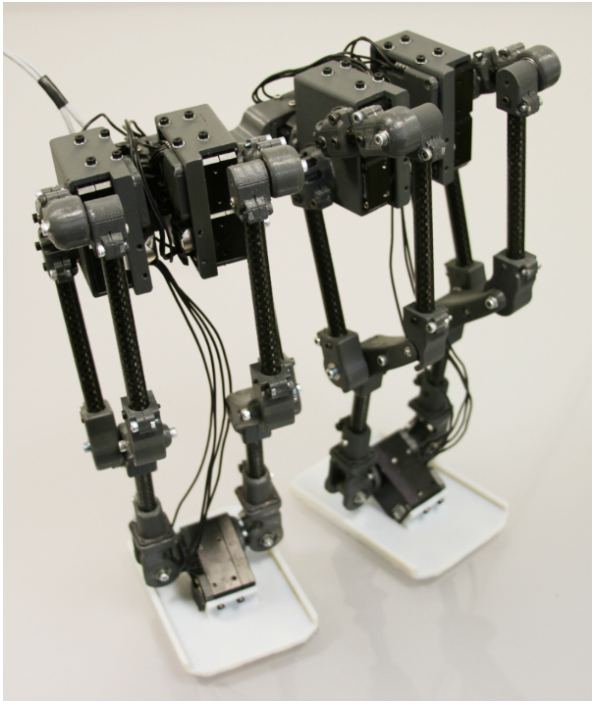

Fig. 1. Bipedal robot lower body assembly

Our review of previous research suggests that low inertia of the leg structure is a common desired feature for robot leg design to realize better dynamic performance. At the same time, most of the leg designs keep anthropomorphic shape for human-like appearance and motion.

Therefore, in pursuit of these characteristics and enhanced dynamic performance to build a bipedal robot can do agile actions such as running or jumping, we proposed a mechanical design for a serial-parallel humanoids leg named *Hybrid Leg* [14].

In our previous work, kinematics of the leg was solved analytically and the performance of the leg design was tested through workspace validation and inverse dynamics analysis. In addition, an early prototype hardware was manufactured to verify the workspace and trajectory tracking performance.

By combining serial mechanism and parallel mechanism to build an entire 6-DOF leg, Hybrid Leg can achieve small

Kevin G. Gim and Joohyung Kim are with Disney Research Los Angeles, Glendale, CA 91201, USA. {kevin.gim, joohyung.kim}@disneyresearch.com

Katsu Yamane was with Disney Research, Pittsburgh, PA, 15213 when the research was conducted. He is now with Honda Research Institute USA, Mountain View, CA 94043, USA. kyamane@honda-ri.com

inertia, large workspace and anthropomorphic structure that resembles the human leg. Hybrid Leg is composed of a pair of 3 DOF chains connected in parallel at the end. Each chain adopts a 5-bar linkage mechanism that realizes the hip pitch and knee pitch motions in order to place the actuators close to the hip. Since these actuators collaborate to generate the knee pitch and hip pitch motions, it is expected to demonstrate an effect similar to the double motor design introduced in the hip and knee pitch joints of some humanoid robot legs [5], [7], [8], [15].

In this paper, we fabricate a second prototype of Hybrid Leg with enhanced components, and assemble the lower body of a bipedal robot using two Hybrid Legs. After evaluating the performance with a single leg, we demonstrate bipedal walking with the bipedal assembly.

This paper is organized as follows. The mechanical design of the single leg prototype and bipedal assembly is presented in Section II. In Section III, we describe the results of performance evaluation including the workspace, maximum foot velocity, and trajectory tracking. Section refsec:walking presents the experimental results of bipedal locomotion. Finally, conclusions and future work are discussed in Section V.

II. Hardware Design

A. Improved Hybrid Leg Design

In our previous work, the first prototype of a serial-parallel 6 DOF Hybrid Leg was fabricated with fully 3D-printed linkages without bearings to demonstrate the idea and test the basic capabilities. While 3D printing allowed us to quickly fabricate a prototype and prove the idea of the design, it was not adequate for evaluating its full performance due to the large friction caused by 3D-printed joint structure and brittle links of the material. In addition, deformation of the 3D-printed linkages, especially when the larger force is applied (i.e., moving fast, supporting body mass with one leg), causes unpredictable kinematic error due to its long linkage structure. Therefore, the second version of Hybrid Leg hardware is fabricated with enhanced durability and dynamic performance to realize bipedal walking locomotion.

The hardware design has been modified to utilize carbon fiber tubes and bearings to improve kinematic accuracy and dynamic characteristic. Specifically, the linkages consist of a 9.525 mm diameter high modulus carbon fiber tube and 3D-printed bearing carriage tips mounted at each end of the tube. The 3D-printed parts was printed by a Stratasys Fortus 450MC printer with ABS-M30 model material.

The new hardware is designed as the leg of a miniature humanoid as it has the identical dimension of the leg of commercialized humanoid robot as in the previous prototype. The link length of the prototype is shown in Table I. The total weight of one leg assembly is 0.9kg which is approximately 0.2kg heavier than the weight of a leg of commercialized humanoids. However, the inertia of moving parts, i.e., femur, tibia and foot, calculated on CAD software is only 71.4% of that of the leg of a toy-sized commercialized robot,

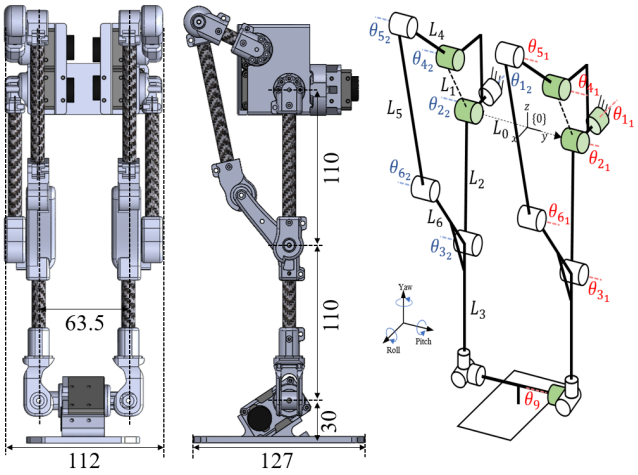

(a) Front and Side view (b) Schematics

Fig. 2. Geometric specification and configuration of a single Hybrid Leg

ROBOTIS OP-3 [16], which is referred for comparison in this paper.

Figure 2 (b) shows a schematic of a single Hybrid Leg. The green colored joints in the schematic are actuated joint while others are passive joint. θ_2 and θ_4 are located on the same link so there is no relative motion between two joints. Also note that L_3 and L_6 are in one rigid body. In a single leg, six servo actuators are installed to control the 6 DOF. Five of the servos (XM430-W350-R) are located in the hip, and one (XM430-W210-R) at the foot.

By connecting two serial chain in parallel, the parallel structure is able to achieve 6 DOF with six active servos.

Overviewing the entire structure, two serial chains are connected in parallel to achieve 6 DOF with 6 active servos. From the top, each serial chain has 3 DOF. One chain is fully actuated by three servos while the other is under-actuated because only hip pitch and knee pitch joints are active and hip roll joint remains passive. Each chain has a hip roll joint θ_1, a hip pitch joint θ_2, and a knee pitch joint θ_3. Note that θ_3 is determined by θ_2 and θ_4 due to the 5-bar linkage mechanism.

By using the 5-bar linkage mechanism for the knee pitch joint, the servo actuator can be placed close to the hip so that it has the advantage of smaller structural inertia of the leg. The kinematic specification of the 5-bar linkages is determined to ensure a range of motion (ROM) sufficient for walking.

At the end of the each serial chain, an ankle structure connects both chains. The connections are made with 3 DOF joints while only one side has an active 1 DOF with a servo. This sixth servo is placed at the foot for the ankle pitch motion. Due to collision between the ankle pitch servo and the ankle structure at the end of the serial chains, ankle roll ROM and yaw ROM are limited as ankle pitch angle increases. Therefore, the ankle servo is attached to the foot with a tilted angle not only to secure more space for angle roll/yaw motion by avoiding collision but also to match its

TABLE I

LINK LENGTH OF THE PROTOTYPE HARDWARE(UNIT: MM)

L_0	L_1	L_2	L_3	L_4	L_5	L_6
63.5	31.26	110	110	47	126.67	50

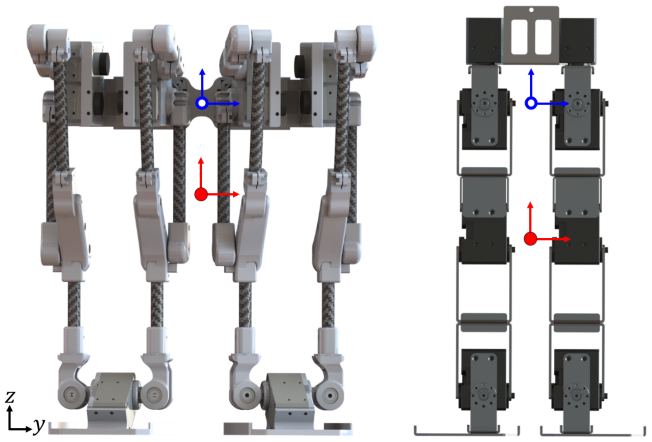

Fig. 3. Front view of a bipedal robot with Hybrid Leg (Left) and a lower body of the commercialize humanoid robot (Right). Origin of each robot are expressed with blue arrows and circle. Red arrows indicate the COM position. The distance from origin to COM for each robot is: Bipedal robot with Hybrid Leg: 60.59mm, Reference humanoids: 98.77mm

kinematic dimension identical to the reference conventional leg.

As the vertical load is distributed to two parallel chain, the hip pitch actuator and knee pitch actuator in one chain collaborate to generate pitch motions. In other words, even though the Hybrid Leg mechanism has the same number of actuators as conventional serial legs, larger actuator power can be assigned to the knee pitch motion and hip pitch motion instead of having identical actuator power in every active joint as in the serial legs.

B. Bipedal Robot Design

We then assemble a bipedal robot using a pair of Hybrid Legs. Left and right legs are designed to be opposite-hand mirrored copies of each other. Including two legs and a pelvis that connects the two legs, the total weight of the lower body assembly is 1.90kg.

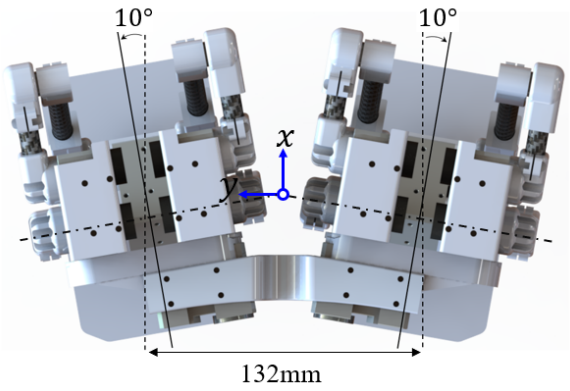

Fig. 4. Top view of the bipedal robot with Hybrid Leg. The origin of the bipedal robot marked with blue arrows is located where the hip pitch joint axis of each leg intersects

Figure 3 shows the biped assembly alongside with a lower body of the reference humanoid robot [16] The red dots indicates the position of COM (Center of Mass) of each lower body. The COM of the bipedal robot is 38 mm, or 15% of the leg length, higher than the COM of the commercialized humanoid robot's lower body.

Since the workspace of the each leg is restricted due to collision between two legs, the width of the lower body needs to be wide to secure workspace. However, wide width of the lower body can make the bipedal robot difficult to balance because it requires a large lateral movement for shifting the weight during walking. In order to make the lower body narrower while achieving a larger workspace, we implement a pelvis with a toe-out offset angle, inspired by the toe-out angle of the human feet. Human feet point outward with some angle in natural posture and movements such as walking and running. According to a study in biomechanics field, the toe-out angle of an average male adult is approximately 11° of the foot progression angle in normal walking gaits [17]. The toe-out angle becomes even larger for a person who has knee osteoarthritis or overweighted person since toe-out gait has an effect of reducing the knee adduction moment [18], [19].

Based on these studies, the pelvis of the bipedal robot with Hybrid leg is designed to connect two legs with 20° of feet angle offset so that each leg point 10° outward at their neutral position. The distance between the center of two foot is 132 mm when the bipedal robot is standing up straight. Compared to the bipedal robot with same foot distance without toe-out angle, the outward hip roll angle limit is increased from 13° to 35° by applying 10° toe-out angle. Figure 4 shows the top view of the bipedal robot with the 10° toe-out angle.

III. PERFORMANCE EVALUATION

A. Workspace

Workspace analysis is performed for a single leg and for the biped robot as well to determine the potential range of walking gaits. Workspace of a single leg is obtained by finding points having a real solution for inverse kinematics at an arbitrary foot position(end-effector position) with a flat orientation sampled at $10mm$ interval with in the range of $-300 \leq x \leq 300$, $-300 \leq y \leq 300$, and $-250 \leq z \leq 0$ in mm. Note that the origin frame of a single leg is located at the middle of hip pitch servos as shown in Fig. 2 (a). When the leg is in a fully stretched posture, the position of the foot is $(0, 0, -250)$. Solutions that exceed the angle limit of each joint are excluded to prevent self-collision. The singularity of 5-bar mechanism is also considered to eliminate infeasible solutions.

By calculating the workspace for both legs considering the toe-out angle and width of the pelvis, workspace of a biped robot can be obtained. The range of hip roll joint is set to be narrower than that of a single leg to prevent the two

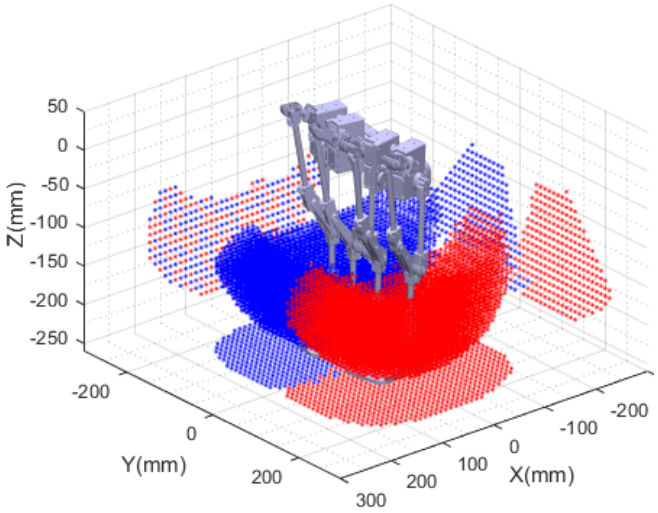

Fig. 5. Workspace of the biped Robot when both feet are in a flat orientation (Red: Workspace of the left leg, Blue: Workspace of the right leg)

legs from colliding each other. The workspace of the bipedal robot is presented in Fig. 5.

B. Maximum Foot Velocity

The maximum x, y, and z velocity of the foot is simulated considering the kinematic constraints and servo speed specifications. When the foot is moving with a constant velocity in the x, y, or z direction, the required servo speed can be computed by differentiating the inverse kinematics solutions [14] for the foot positions sampled at $0.001sec$. If any of the servo speed reaches the no-load speed of the servo provided by the manufacturer, the foot velocity is considered to be the maximum.

The resulting plots for the joint velocity at the maximum foot velocity in x,y, and z directions are presented in Fig. 6. In Fig. 6 (a), velocity of the knee pitch servo ($\dot{\theta}_4$, $\dot{\theta}_5$) reaches the no-load speed while the foot is moving from backward to forward ($(-100, 0, -200)$ to $(100, 0, -200)$) with a velocity of 465.12 mm/s at $x = 0$ mm. Similarly, the hip roll servo speed($\dot{\theta}_1$) reaches the no load speed while the foot is traveling from left to right ($(0, -100, -200)$ to $(0, 100, -200)$) with 816.32 mm/s foot velocity at $y = 0$ mm as presented in Fig. 6 (b). For Z movement, the maximum reachable velocity is 333.33 mm/s at $z = -220$ mm while the foot is moving from (0,0,-140) to (0,0,-240) as presented in Fig. 6 (c). The lower the foot position, the faster servo speed is required to achieve the same z velocity. Therefore, the foot can move with faster velocity when the foot position is higher. For example, the maximum z direction velocity when the foot height is -200 mm is 666.67 mm/s. When there is no x and y displacement, the hip joint movement is identical to that of a serial leg with the same dimension.

C. Trajectory Tracking Performance Experiment

We conduct hardware experiments to evaluate the trajectory tracking performance when there is no external force applied to the foot. The reference foot trajectory is given as

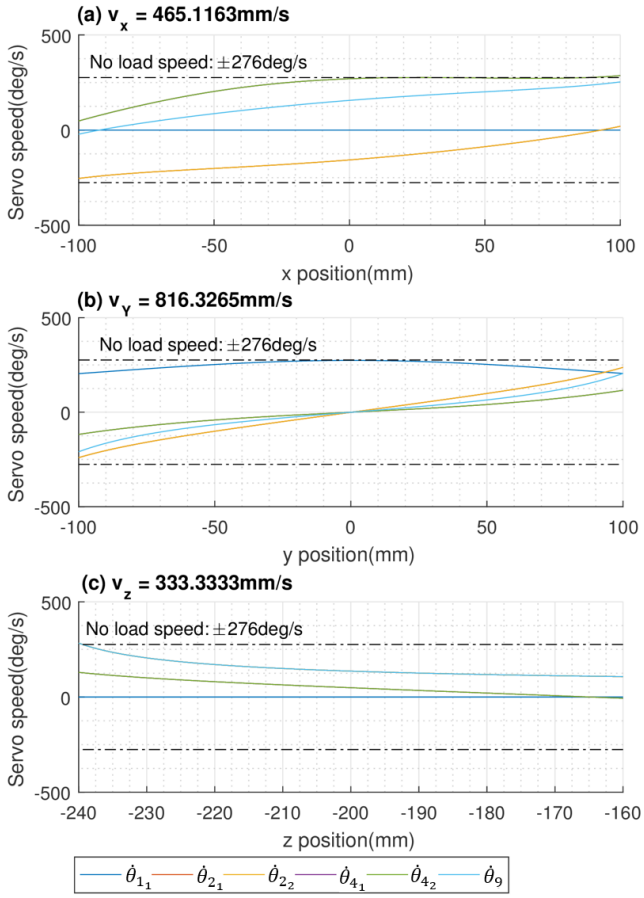

Fig. 6. Velocity of each servo for foot position under a constant velocity of (a) $V_x = 465.12mm/s$, (b) $V_y = 816.32mm/s$, (c) $V_z = 333.33mm/s$.

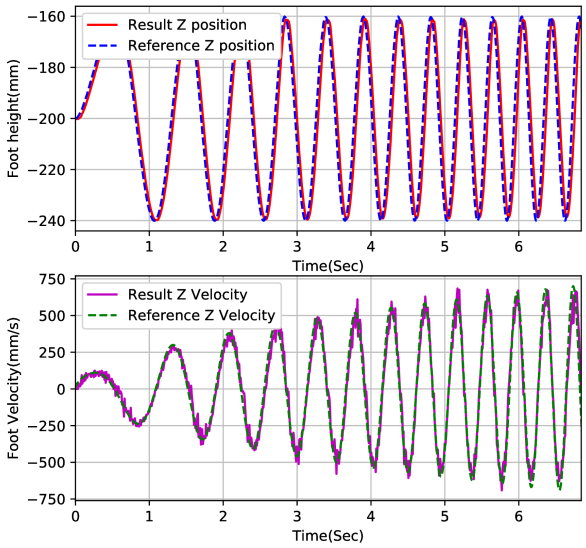

Fig. 7. Results of trajectory tracking performance evaluation.

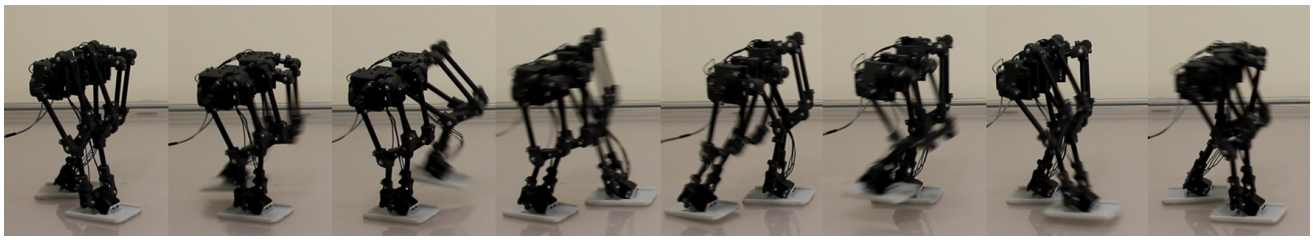

Fig. 8. Snapshots of forward walking experiments. This shows a stride of walking, captured in every 0.2 s

a sine wave with -200 mm offset, 80 mm amplitude while the foot maintains the nominal orientation. The frequency of the sine wave is increased at each cycle so that the peak foot velocity increases over time. The trajectory has 10 cycles with a duration of 7 s, and the maximum velocity at the last cycle is 660 mm/s which is set to be lower than the maximum velocity obtained by the kinematic simulation, 666.67 mm/s, when the foot position is at $z = -200$ mm. The trajectory is sampled at 0.005 s and the joint angle commands given to the servos are computed from the foot position by inverse kinematics. The servos are PID position control with 1 KHz loop time. From the recorded servo angle output, the actual z position and velocity are calculated by forward kinematics. The results are presented in Fig. 7. As shown in the result plot, the foot is able to track position command accurately until the foot is moving with a maximum velocity derived by the kinematic simulation.

IV. Bipedal Locomotion

The bipedal walking performance of the bipedal robot with Hybrid Leg is tested on the developed hardware. To validate the prototype hardware capability, a bipedal walking motion is implemented by manually generating the foot trajectory. The test walking gait is planned with a simplified approach of separating the sagittal and lateral movements. We generated the decoupled movements and modified the timing of swing phase by experiments. The generated gait has 0.8 s step time and 175 mm step length, which is as large as 70% of the total leg length. The toe-out angle of 10° is maintained during the walking motion. The bipedal walking performance was evaluated through a forward walking motion of 4 steps on a flat office desk. Fig. 8 shows the two out of the four steps captured at 0.2 s interval. Please refer the supplementary video to see the robot's walking motion.

Figure 9 presents the walking experiment result including the reference foot trajectory and joint angle input/output of each servo actuators. Note that the feet touch the ground when their z position is -230 mm in the foot trajectory plot. The joint angle plot shows that the joints can track the reference trajectories accurately even when the leg supports the robot's weight.

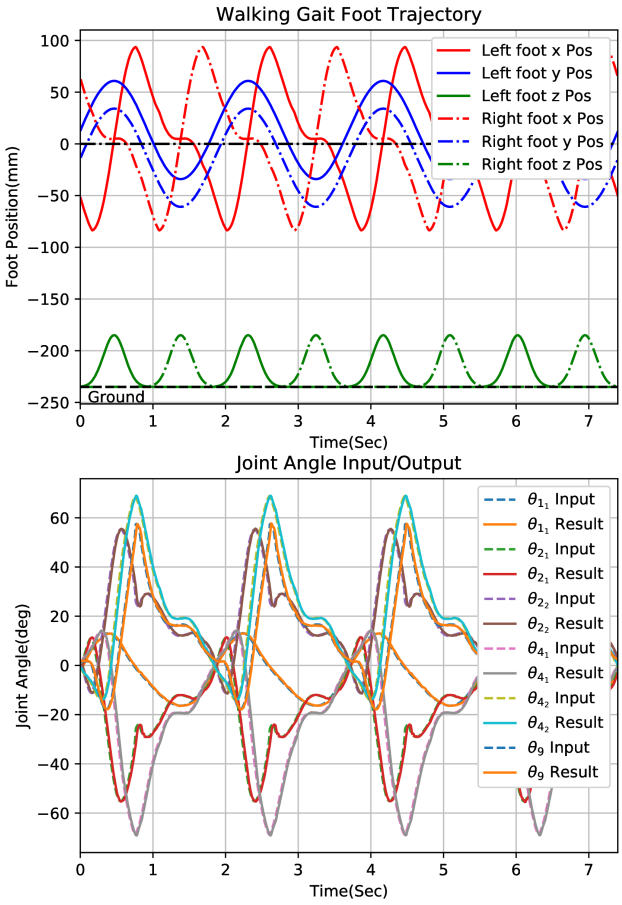

Fig. 9. Experimental results of forward walking. The above graph shows the relative position of each leg from the origin at pelvis. The graph below shows reference angles and measured angles of servos while walking.

V. Conclusions and Future Work

In this paper, we presented the design and performance of a bipedal robot using the Serial-Parallel Hybrid Leg mechanism. The Hybrid Leg was fabricated with carbon fiber tubes and bearings to improve structural rigidity and accuracy while supporting its weight. A pair of Hybrid Legs is assembled together to form the lower body of a bipedal robot. In the assembly, we adopt a pelvis link with yaw angle offset to enlarge the feet workspace, inspired by the toe-out angle of the human feet. The workspace and range of velocity are analyzed in simulation and verified with hardware experiments. A simple forward walking gait is implemented and the developed robot successfully achieve the forward walking by tracking the given reference trajectories.

As our future work, we are planning to fabricate all the linkage with carbon fiber 3D printing. Even if the hardware

design of our Hybrid Leg has been improved comparing to the previous version, it can be further enhanced by substituting 3D printed ABS material part and carbon fiber tube part with one-piece part. Also, we are planning to make this robot as a standalone robot. In this work, the robot was tethered with wires to get control commands and power. We will add an embedded computer, a battery and sensors to make it freely locomote indoor environments.

In the software side, an advanced walking algorithm will be necessary for indoor locomotion. From the results in Section III, we found that the developed hardware has enough speed and power for jumping or running. So we will explore more agile locomotion with this robot.

REFERENCES

[1] Y. Sakagami, R. Watanabe, C. Aoyama, S. Matsunaga, N. Higaki, and K. Fujimura, "The intelligent asimo: System overview and integration," in *Intelligent Robots and Systems, 2002. IEEE/RSJ International Conference on*, vol. 3. IEEE, 2002, pp. 2478–2483.

[2] K. Kaneko, F. Kanehiro, M. Morisawa, K. Miura, S. Nakaoka, and S. Kajita, "Cybernetic human hrp-4c," in *Humanoid Robots, 2009. Humanoids 2009. 9th IEEE-RAS International Conference on*. IEEE, 2009, pp. 7–14.

[3] I. Ha, Y. Tamura, H. Asama, J. Han, and D. W. Hong, "Development of open humanoid platform darwin-op," in *SICE Annual Conference (SICE), 2011 Proceedings of*. IEEE, 2011, pp. 2178–2181.

[4] J. Kim, Y. Lee, S. Kwon, K. Seo, H. Kwak, H. Lee, and K. Roh, "Development of the lower limbs for a humanoid robot," *2012 IEEE/RSJ International Conference on Intelligent Robots and Systems*, pp. 4000–4005, 2012.

[5] J. Lim, I. Lee, I. Shim, H. Jung, H. M. Joe, H. Bae, O. Sim, J. Oh, T. Jung, S. Shin, K. Joo, M. Kim, K. Lee, Y. Bok, D.-G. Choi, B. Cho, S. Kim, J. Heo, I. Kim, J. Lee, I. S. Kwon, and J.-H. Oh, "Robot System of DRC-HUBO+ and Control Strategy of Team KAIST in DARPA Robotics Challenge Finals," *Journal of Field Robotics*, vol. 34, no. 4, pp. 802–829, jun 2017.

[6] S. G. McGill, S. J. Yi, H. Yi, M. S. Ahn, S. Cho, K. Liu, D. Sun, B. Lee, H. Jeong, J. Huh, D. Hong, and D. D. Lee, "Team THOR's Entry in the DARPA Robotics Challenge Finals 2015," *Journal of Field Robotics*, vol. 34, no. 4, pp. 775–801, may 2017.

[7] K. Kaneko, M. Morisawa, S. Kajita, S. Nakaoka, T. Sakaguchi, R. Cisneros, and F. Kanehiro, "Humanoid robot HRP-2Kai - Improvement of HRP-2 towards disaster response tasks," *IEEE-RAS International Conference on Humanoid Robots*, vol. 2015-Decem, pp. 132–139, 2015.

[8] Y. Kakiuchi, K. Kojima, E. Kuroiwa, S. Noda, M. Murooka, I. Kumagai, R. Ueda, F. Sugai, S. Nozawa, K. Okada, and M. Inaba, "Development of humanoid robot system for disaster response through team NEDO-JSK's approach to DARPA Robotics Challenge Finals," *IEEE-RAS International Conference on Humanoid Robots*, vol. 2015-Decem, pp. 805–810, 2015.

[9] C. G. Atkeson, B. P. W. Babu, N. Banerjee, D. Berenson, C. P. Bove, X. Cui, M. DeDonato, R. Du, S. Feng, P. Franklin, M. Gennert, J. P. Graff, P. He, A. Jaeger, J. Kim, K. Knoedler, L. Li, C. Liu, X. Long, T. Padir, F. Polido, G. G. Tighe, and X. Xinjilefu, "No falls, no resets: Reliable humanoid behavior in the darpa robotics challenge," in *2015 IEEE-RAS 15th International Conference on Humanoid Robots (Humanoids)*, Nov 2015, pp. 623–630.

[10] S. Lohmeier, T. Buschmann, and H. Ulbrich, "Humanoid robot LOLA," *Proceedings - IEEE International Conference on Robotics and Automation*, pp. 775–780, 2009.

[11] N. G. Tsagarakis, D. G. Caldwell, F. Negrello, W. Choi, L. Baccelliere, V. Loc, J. Noorden, L. Muratore, A. Margan, A. Cardellino, L. Natale, E. Mingo Hoffman, H. Dallali, N. Kashiri, J. Malzahn, J. Lee, P. Kryczka, D. Kanoulas, M. Garabini, M. Catalano, M. Ferrati, V. Varricchio, L. Pallottino, C. Pavan, A. Bicchi, A. Settimi, A. Rocchi, and A. Ajoudani, "WALK-MAN: A High-Performance Humanoid Platform for Realistic Environments," *Journal of Field Robotics*, vol. 34, no. 7, pp. 1225–1259, oct 2017.

[12] J. A. Grimes and J. W. Hurst, "the Design of Atrias 1.0 a Unique Monopod, Hopping Robot," pp. 548–554, 2012.

[13] Agility Robotics, "Cassie." [Online]. Available: http://www.agilityrobotics.com/robots/

[14] K. Gim, J. Kim, and K. Yamane, "Design of a Serial-Parallel Hybrid Leg for a Humanoid Robot," in *IEEE International Conference on Robotics and Automation*. IEEE, 2018.

[15] Y. Ito, S. Nozawa, J. Urata, T. Nakaoka, K. Kobayashi, Y. Nakanishi, K. Okada, and M. Inaba, "Development and verification of life-size humanoid with high-output actuation system," *Proceedings - IEEE International Conference on Robotics and Automation*, pp. 3433–3438, 2014.

[16] ROBOTIS, "Op3." [Online]. Available: http://www.robotis.us/robotis-op3/

[17] H. Koblauch, T. Heilskov-Hansen, T. Alkjær, E. B. Simonsen, and M. Henriksen, "The Effect of Foot Progression Angle on Knee Joint Compression Force during Walking," *Journal of Applied Biomechanics*, vol. 29, no. 3, pp. 329–335, jun 2013.

[18] R. Debi, A. Mor, O. Segal, G. Segal, E. Debbi, G. Agar, N. Halperin, A. Haim, and A. Elbaz, "Differences in gait patterns, pain, function and quality of life between males and females with knee osteoarthritis: a clinical trial," *BMC Musculoskeletal Disorders*, vol. 10, no. 1, p. 127, dec 2009.

[19] M. Masaun, P. Dhakshinamoorthy, and R. S. Parihar, "Comparison of Calcaneal Eversion, Gastrocnemius Extensibility and Angle of Toe-Out between Normal and Overweight Females," *The Foot and Ankle Online Journal*, aug 2009.